Polymer Degradation and Stability 109 (2014) 307–318

Contents lists available at ScienceDirect

Polymer Degradation and Stability

journal homepage: www.elsevier.com/locate/polydegstab

Identification and characterization of plastics from small appliances and kinetic analysis of their thermally activated pyrolysis

Lorenzo Cafiero [a, *], Eugenio Castoldi [a], Riccardo Tuffi [a], Stefano Vecchio Ciprioti [b, *]

[a] Department of Environmental Technologies, ENEA – Casaccia Research Center, Via Anguillarese 301, 00123, S. Maria di Galeria, Rome, Italy
[b] Department S.B.A.I., Sapienza University of Rome, Via del Castro Laurenziano 7, I-00161 Rome, Italy

ARTICLE INFO

Article history:
Received 17 April 2014
Received in revised form
28 June 2014
Accepted 2 August 2014
Available online 12 August 2014

Keywords:
WEEE
Mixed plastic waste
Acrylonitrile-butadiene-styrene plastics
High impact polystyrene
Polybutadiene terephthalate
Pyrolysis kinetics

ABSTRACT

The first step consisted in a field investigation carried out in Waste Electric and Electronic Equipment (WEEE) treatment plants coupled with a bibliographic product analysis and FT-IR spectroscopy polymers identification. Three main polymers of the thermoplastic fraction of small appliances were identified: in the external cases it was possible to find acrylonitrile-butadiene-styrene (ABS) and high impact polystyrene (HIPS), while polybutadiene terephthalate (PBT) was contained in the printed circuit boards (PCBs). Taking into account this identification, a ternary polymer mixture of ABS-HIPS-PBT was prepared as a representative sample of the thermoplastic fraction contained in WEEE (real WEEE sample). From the thermal characterization (proximate and ultimate analysis, high heating value (HHV) direct measurement and Energy-Dispersive-X-Ray-Fluorescence analysis (ED-XRF)) the only polymer whose properties sensibly differ from the analogous virgin polymer is the one contained in PCBs.

A kinetic analysis of pyrolysis occurring on the three components and on their ternary mixture was performed using a thermogravimetry (TG) apparatus in argon atmosphere under non isothermal conditions. Triplicates of TG experiments at four heating rates of 2, 5, 10 and 15 K min^{-1} were carried out and two different model-free approaches were adopted, namely the Kissinger and Ozawa-Flynn-Wall methods in order to determine the activation energy E (as a single mean value or as a function of the degree of conversion α). The conversion dependencies of both activation energy and pre-exponential factors were determined as well as the reaction model, representing the reaction mechanism. The suitability of the models selected was tested using the Akaike's Information Criteria (AIC) score, being the geometric model R3 the best found for pyrolysis of ABS, HIPS and real WEEE samples, while PBT sample showed an uncertainty between the R3 and the diffusion D2 model. The reaction time values to achieve the maximum pyrolysis rate in the three main components and in the real WEEE sample were also calculated.

1. Introduction

According to the Statistical Office of the European Union (EUROSTAT), Waste of Electric and Electronic Equipment (WEEE) generated in the European Union (EU) amounts to three times as much as the quantity properly collected and managed in Europe [1]. A recovery rate from 70% to 80%, either in terms of energy or materials, is required to all EU Member States [2]. The plastic fraction contained in WEEE accounts for about 30% [3] and consequently its proper management may give a significant contribution to achieve the EU targets. Furthermore, the Italian Legislation in relation with the EU Landfill Directive [4] forbids the landfilling of waste with a Lower Heating Value (LHV) exceeding 13 MJ kg^{-1}. On the other hand, the mechanical recycling of the plastic fractions of WEEE is problematic for two substantial reasons: the great heterogeneous composition and the content of hazardous substances. The first issue is even more severe for small appliances which include more than 15 different polymeric categories whether homopolymers, copolymers, blends, because of the large number of different applications; mechanical recycling cannot handle mixed plastics waste with a consistent content in inert and metal fraction which may be present in WEEE [5,6].

Furthermore, most applications require polymer additivation such as plasticizers, stabilizers, flame retardants, which enhance their heterogeneity and can be or generate hazardous compounds

* Corresponding authors.
E-mail addresses: lorenzo.cafiero@enea.it (L. Cafiero), stefano.vecchio@uniroma1.it (S. Vecchio Ciprioti).

http://dx.doi.org/10.1016/j.polymdegradstab.2014.08.001
0141-3910/

to the environment [7]. Although Restriction of Hazardous Substances (RoHS) Directive [8] limited the use of these compounds since July 2006, old EEE manufactured before that date are still on use as they are long life products (generally up to 10 a year life span). To conclude, even if plastics reprocessing is technically feasible, ecological-impact studies in the Netherlands and Germany [9] have demonstrated that there is a limit of 15%–18% to the amount of thermoplastic waste that can be mechanically recycled with environmental benefits. Further mechanical recycling requires a relatively major effort that annuls any environmental gain. This means that the majority of the remaining waste must be recycled by other techniques.

Thermal techniques in general and pyrolysis in particular allow dealing with the heterogeneity and complex composition of mixed plastics [5–6] and classifying waste components to be used for energy generation [10]. As far as the other thermal treatments are concerned, pyrolysis presents the further advantages of yielding derivative petro-based chemicals to be exploited as feedstock or fuel and generating a solid residual stream, whose chemical properties remain unaltered and prone to be recovered, such as metals and fibreglass [5]. Furthermore, reduced volumes of gas are associated to pyrolysis [9] and sulphur and nitrogen oxides and polychlorinated dibenzodioxines (PCDD) production is limited as well [11–13].

Only heterogeneous recycling is feasible for mixed plastics, and metals and inorganics can be found in the solids present after pyrolysis that belong to the raw material. Liquid pyrolysis products may vary significantly depending on the components of the WEEE pyrolysed. Gases WEEE pyrolysis products are mainly composed by low-molecular weight hydrocarbons and significant amounts of CO and CO_2 [6]. Previous studies carried out by De Marco and coworkers with other plastic wastes [14,15] (used car tyres, automobile shredder residues, etc.) demonstrated that in the mentioned installation, 773 K is the optimum temperature for treating polymeric wastes by pyrolysis.

The set-up of a pyrolysis process and its possible scale-up requires carrying out a preliminary kinetic study in order to find the reaction time of decomposition [16]. Kinetic investigation on pyrolysis occurring in mixed WEEE samples from small appliances was carried out using a procedure recently applied for other different kinds of materials, like imidazole derivatives or lanthanide complexes as well as for triglycerides contained in extra-virgin olive oils [17–19].

As far as the interpretation of kinetic results is concerned, Simon suggested that kinetic parameters represent apparent quantities without a mechanistic interpretation [20]: the parameters cannot be used for any theoretical considerations, but they enable modelling the processes for other temperature regimes beside those applied in the measurements. In the past, many authors examined the pyrolysis of WEEE as a whole [6,11,21,22], but they did not consider the process occurring in each component. On the other hand, a great deal of data on pyrolysis kinetics and thermal stability comes from studies applied to single commercial or virgin polymers [23–28], but the novelty and the most important aim of this study is the identification and thermal characterization of the most representative thermoplastic components extracted from WEEE found in small appliances (housing and printed circuit boards, PCB) and their mixture. Our attention was focused on the analysis of their pyrolysis kinetics using reliable kinetic methods. Furthermore, literature data concerning the thermal decomposition of virgin thermoplastic polymers usually contained in scrap PCBs (i.e. polybutadiene-terephthalate (PBT), nylon 6.6, polyphenylene sulfide) are quite scarce [29,30] and, according to our knowledge, no papers are found on the kinetic analysis of pyrolysis occurring in these materials when they are contained in electronic wastes. The results obtained were presented in terms of the so-called kinetic triplet that means providing three parameters: the values of activation energy and pre-exponential factor associated to pyrolysis process (actually a set of values as a function of the extent of transformation) along with a model function $f(\alpha)$ that is directly connected to the pyrolysis mechanism. In addition, the Akaike's Information Criterion (AIC) was considered since it is recognized by many authors [31–33] to be a reliable tool for selecting the most appropriate reaction model among those considered (13 in this study) using a severe statistical criterion. Furthermore, this procedure enables also to estimate the reaction time to achieve a given conversion at a reference temperature. The results obtained will contribute in optimizing pyrolysis tests for WEEE plastics and leading up to a subsequent experimental work to determine a particular scale of operation, with reference to a continuously operated bench-scale rotary kiln. Finally, as far as the reaction time is concerned, these values can be used to obtain the general energy balance equation of the pyrolysis process, and allow calculating the minimum residence time for a pyrolysis reactor to achieve a complete transformation.

2. Experimental

2.1. Materials and methods

Mixed plastics from small appliances were supplied by WEEE selection and treatment plants set in Central Italy. The selection of samples used in this work was performed by an integrated approach based on the results of product analysis provided by literature [34,35] and the identification of polymers in WEEE samples by infrared spectroscopy; the selection criteria were established by the polymer abundance both in housing and in PCBs. According to what it was described in previous papers [34,35], the three main housing constituents appeared to be acrylonitrile-butadiene-styrene (ABS), polypropylene (PP) and high-impact polystyrene (HIPS) with percentages of 37, 29 and 19% w/w respectively; on the other hand, the group of macromolecules contained in PCBs was led by PBT, showing a percentage of 1.7% on the whole amount. The selected plastic parts came from shredded mixtures of various personal computer brands; in particular, FT-IR spectroscopy allowed to identify HIPS in the personal computer external housing and was coded as “PC”, ABS in the keyboard case and was coded as “Keyb”, PBT in the RAM slot and was coded as “Black slot”.

A further sample, representative of the WEEE plastics (denoted as “Real WEEE”), was prepared as a ternary mixture of the above-mentioned plastic samples, with a normalized composition based on the commercial analysis reported above (64, 33 and 3% w/w for Keyb, PC and Black slot, respectively). These plastic samples were subjected to the proximate and ultimate analysis and to the determination of the LHW. These analyses were extended to virgin polymers for comparison. Each measurement was performed with at least three replicates for each sample.

Finally, pyrolysis kinetic tests were carried out to determine the Arrhenius parameters associated with the process.

Prior to any test, the raw materials were reduced to a particle size lower than 0.35 mm. Size reduction is very important for pyrolysis kinetic experiments, as a diameter particle $\leq$0.35 mm is sufficient to assume that no thermal gradients take place inside the particles during the occurrence of pyrolysis as well as to ensure an even distribution of the different components (plastic mixture), which the samples are comprised of by mechanical mixing [21]. If necessary, liquid nitrogen was used to decrease significantly the sample temperature in order to take advantage of the mechanical properties of plastic materials that become brittle enough to be easily milled.

2.2. Fourier transformed infrared spectroscopy

Fourier transformed infrared spectroscopy (FT-IR) measurements were carried out with a IRAffinity-1 FT-IR Shimadzu apparatus. The surface was analysed using a single reflection attenuated total reflectance (ATR) technique performed by a MIRacle 10 Accessory Pike Technologies. Forty-five scans between 4600 and 600 cm^{-1} were averaged for each spectrum at intervals of 1 cm^{-1}.

2.3. Proximate analysis

Experiments for the determination of humidity, volatile matter, fixed carbon and ash content were carried out using a TGA 2950 macro thermobalance (TA Instruments) with about 1 g of sample according to the US technical specification ASTM D7582 − 12 adopted for coal and coke. The temperature program adopted is shown in Table 1. The organic matter is the sum of the volatile fraction plus the fixed carbon (determined by difference), while the ash content represents the inorganic matter.

2.4. Elemental analysis

The weight percentage of carbon, nitrogen, hydrogen and sulphur found in the sample were determined simultaneously using a Macro VARIO Cube Elemental Analyser. By introducing specific modules it is possible the direct measurement of oxygen. Analysis of chlorine and bromine to determine their content was performed following the European technical specification CEN/TS 15408 [36], which envisages the following procedure: flue gas from the combustion chamber of a C5000 Berthelot-Mahler Calorimeter IKA was allowed to pass through a sampling bottle filled with a $NaHCO_3/Na_2CO_3$ buffer solution to be further analysed through a 883 Basic IC plus Ion Cromatographer Metrohm equipped with a Metrosep A Supp 4-250/4.0 anionic column for determining bromine and chlorine content. In the unique case of black slot sample, because of its high ash content, the presence of minor elements was investigated through the Energy Dispersive X-ray Fluorescence (EDXRF) technique, using a EDX-720 Shimadzu Spectrometer equipped with an Rh-lined X-ray tube under a voltage of 15–50 kV in air atmosphere.

2.5. Calorimetric determination of LHV

The low heating value (LHV) was obtained by measuring directly the high heating value (HHV) by C5000 Berthelot-Mahler Calorimeter IKA applying the following expression:

$$\mathrm{LHV} = \mathrm{HHV} - 9(\mathrm{HyC}) - 2.5(\mathrm{HuC}) \quad (1)$$

where HyC and HuC are the hydrogen and the humidity content, respectively, expressed as percentages in the sample. About 0.5 g of powder was weighed into a crucible and placed inside a stainless steel container. The decomposition vessel was filled with 3 MPa of technical oxygen and ignited. The heat created during the burning process of organic matter was determined using the adiabatic measurement procedure. The calibration consisted in assessing the heat capacity of the decomposition vessel by burning tablets of certified benzoic acid.

LHV is an estimation of the maximum energetic potential extractable from the examined materials and allows having an order of magnitude of the generated pyrolysis products.

2.6. Thermogravimetry

In order to examine the thermal behaviour and analyse the pyrolysis kinetics of the components and mixture tested thermal analysis experiments were carried out on about 10 mg of a solid powder sample using a SETARAM 92-16.18 thermogravimetric (TG) apparatus in the temperature range between 298 and 973 K using different heating rates (2, 5, 10 and 15 K min^{-1}) under an argon carrier gas of 30 mL min^{-1} flow rate. The instrument was calibrated by melting some very pure standard metals in the temperature ranges around 430 K (for indium) and 1235 K (for silver) at all four heating rates considered in this study and a temperature uncertainty of 0.5 K was estimated. Because of the buoyancy effect, a preliminary"blank experiment" was carried out before each run.

2.7. Pyrolysis kinetic theory and procedure

Pyrolysis kinetics was studied by processing non-isothermal TG data by applying two model-free multiple-heating rate methods for the calculation of the kinetic parameters: Kissinger [37] and the isoconversional one of Ozawa-Flynn-Wall [38,39]. All isoconversional methods are based on the isoconversional principle that the reaction rate at constant extent of conversion is only a function of temperature. The transformation progress involving solid substances is usually represented as a function of both temperature T and degree of conversion α, being $\alpha = (m_i - m_t)/(m_i - m_f)$, where m_i is the initial mass sample, m_t is the mass sample at actual time and m_f is the sample mass at the final time. This basic equation, rigorously valid for a single-step process only, is commonly represented as follows:

$$d\alpha/dt = k(T)f(\alpha) \quad (2)$$

where $k(T)$ is the rate constant and $f(\alpha)$ is a differential model function. If the $k(T)$ term is expressed by the Arrhenius equation, after rearrangement Eq. (2) takes the form:

$$d\alpha/dt = A \exp(-E_a/RT) f(\alpha) \quad (3)$$

where E_a is the activation energy (in kJ mol^{-1}), A is the pre-exponential factor (in min^{-1}) and R is the universal gas constant in J mol^{-1} K^{-1}. In non-isothermal experiments the most commonly used temperature program is the one in which the time dependence of temperature, namely the heating rate $\beta = dT/dt$, is constant. Thus, Eq. (3) can be rewritten as follows:

$$d\alpha/dT = (A/\beta) \exp(-E_a/RT) f(\alpha) \quad (4)$$

Since the mechanism of thermal decomposition occurring in WEEE materials is expected to be complex and not representable by

Table 1
Procedure of TG experiments for the proximate analysis.

Parameter	N_2 at 70 ml min^{-1}				Air at 90 ml min^{-1}			
	T_i (K)	T_f (K)	$\beta = dT/dt$ (K min^{-1})	Δt (min)	T_i (K)	T_f (K)	$\beta = dT/dt$ (K min^{-1})	Δt (min)
Humidity	308.15	378.15	20	3.5				
	378.15	378.15	0	15				
Volatile matter	378.15	1173.15	20	40				
	1173.15	1173.15	0	5				
Ash					1173.15	1173.15	0	30

a single mathematic expression $f(\alpha)$, model-free methods, which enable determining the E_a and A without the selection of the most suitable model function, may be considered to be preferable leading to more reliable and accurate results.

The model free methods adopted in this study use TG data recorder at several heating rates. Because of its easy use, the first method used was that of Kissinger [37], that enable to determine mean values of E_a (for the whole pyrolysis process) from the slope of the regression line derived by plotting $\ln(\beta_i/T_m^2)$ *vs.* $1000/T_m$ according to the following equation:

$$\ln\left(\beta_i \Big/ T_{m,i}^2\right) = \text{Const} - \left(E_a/RT_{m,i}\right) \tag{5}$$

where the subscript i refers to each experiment at a given heating rate, $T_{m,i}$ corresponds to the maximum reaction rate at each fixed heating rate (α_{max}, for which $d^2\alpha/dt^2 = 0$), which corresponds to the peak temperature of the first-order derivative of the TG (DTG) curve.

Among the model free methods, those denoted as "isoconversional" usually provide the most accurate results by evaluating the kinetic parameters at progressive values α if the isoconversional principle (reaction rate at a fixed value α is only a function of temperature) is accomplished. In fact, if the logarithmic form of Eq. (2) is differentiated with respect to temperature at α = constant, it yields:

$$\left[\partial(d\alpha/dt)\Big/\partial T^{-1}\right]_\alpha = \left[\partial \ln k(T)\Big/\partial T^{-1}\right]_\alpha + \left[\partial \ln f(\alpha)\Big/\partial T^{-1}\right]_\alpha \tag{6}$$

Since $f(\alpha)$ is constant at a fixed value of α, the second term of the right-hand side of Eq. (6) is zero. Thus, the temperature dependence of the logarithm of the reaction rate enables the E_a value to be determined at a given value of α through the following equation:

$$\left[\partial \ln(d\alpha/dt)\Big/\partial T^{-1}\right]_\alpha = -\left(E_a/R\right)$$

To verify if the Arrhenius parameters associated to the thermally activated pyrolysis occurring in the WEEE materials examined vary with the extent of reaction the isoconversional method of Ozawa and/or Flynn-Wall (OFW) [38,39] was applied using the following equation:

$$\ln(\beta_i) = \text{Const} - 1.052\left(E_\alpha/RT_{\alpha,i}\right) \tag{7}$$

where β_i indicates the values of heating rate adopted (in K min^{-1}), E_α the activation energy value at each value of α and $T_{\alpha,i}$ the temperature to reach a given value of α at each heating rate. Reliability of Eq. (7) is based on the validity of Doyle's approximation [40] ($20 \le x_i \le 60$, where $x_i = 10^3\ E_\alpha/RT_\alpha$), otherwise inaccurate values of E_α may result [41]. For each fixed value of α, the corresponding E_α values are determined from the slope of the regression line obtained by plotting $\ln(\beta_i)$ *vs.* $(T_{\alpha,i})^{-1}$.

Prediction of lifetime for a tested material is another crucial point worth to be analysed and critically discussed. The knowledge of the kinetic triplet (E_a, A and $f(\alpha)$) is mandatory and can be determined using both isothermal or non-isothermal experiments. The most appropriate reaction model and the α-dependence of pre-exponential factor ($\ln A_\alpha$) can be accurately determined only in the case of processes occurring approximately in a single-step, for which it can be expected that activation energy does not vary appreciably over the entire range of the extent of conversion α, by combining the results of isoconversional (model-free) and model-fitting methods (Coats-Redfern [42] in this study). By applying a model-fitting method to the results obtained by a single-heating rate experiment a pair of Arrhenius parameters can be obtained for each reaction model considered using the following equation [41,42]:

$$\log\left[g_i(\alpha)\Big/T^2\right] = \log\left[(AR/\beta E)(1 - 2RT/E)\right] - E/(2.303RT) \tag{8}$$

Even if wide ranges of values are found for both parameters when all the reaction models are considered, a strong linear correlation denoted as compensation effect is found between them in the following form:

$$\ln A_i = aE_i + b \tag{9}$$

where the superscript i refers to each of all the reaction model. Once a and b parameters have been determined at each heating rate using a linear regression procedure (least square method), these values were replaced in Eq. (9) by their mean values $\langle a\rangle$ and $\langle b\rangle$ while the E_i values were replaced by the isoconversional values of E_α to determine the corresponding values of $\ln A_\alpha$ for each given value of α according to Eq. (10):

$$\ln A_\alpha = \langle a\rangle E_i + \langle b\rangle \tag{10}$$

Since the application of this method requires negligible variation of E (and of course of $\ln A$) with α, then average values E_0 and A_0 can be considered to determine the reaction model. The integral function $g(\alpha)$ is reconstructed numerically at each value of α, by replacing the E and A values in Eq. (8) with the average values E_0 and A_0, and the upper limit of the temperature integral in the right-side hand T with T_α (corresponding to the value a given value of α), yielding:

$$\log\left[g(\alpha)\Big/T_\alpha^2\right] = \log\left[(A_0R/\beta E_0)(1 - 2RT'/E_0)\right] - E_0/(2.303RT_\alpha) \tag{11}$$

where T_α is the temperature corresponding to a certain α at a given heating rate β and T′ is the average temperature in the α range used for computation of E_0. For any value of T_α, a numerical value of $g(\alpha)$ is calculated at any given value of α. The trend of numerical values of $g(\alpha)$ vs. α so obtained is compared with those theoretically determined according to the expressions found in the last column of Table 2. The best match between the former and the latters identify the most appropriate model function. Since selection of the best model function was found to be difficult in this case, the AIC method [31] was considered. It consists of assessing the following formula:

Table 2
The most commonly used kinetic models for kinetic analysis of thermally stimulated processes.

	Reaction model	Code	$f(\alpha)$	$g(\alpha) = \int d\alpha/f(\alpha)$
1	Power law	P4	$4\alpha^{3/4}$	$\alpha^{1/4}$
2	Power law	P3	$3\alpha^{2/3}$	$\alpha^{1/3}$
3	Power law	P2	$2\alpha^{1/2}$	$\alpha^{1/2}$
4	Power law	P2/3	$(2/3)\alpha^{-1/2}$	$\alpha^{3/2}$
5	One-dimensional diffusion	D1	$1/(2\alpha)$	α^2
6	Mampel (first-order)	F1	$1-\alpha$	$-\ln(1-\alpha)$
7	Avrami-Erofeev	A4	$4(1-\alpha)[-\ln(1-\alpha)]^{3/4}$	$[-\ln(1-\alpha)]^{1/4}$
8	Avrami-Erofeev	A3	$3(1-\alpha)[-\ln(1-\alpha)]^{2/3}$	$[-\ln(1-\alpha)]^{1/3}$
9	Avrami-Erofeev	A2	$2(1-\alpha)[-\ln(1-\alpha)]^{1/2}$	$[-\ln(1-\alpha)]^{1/2}$
10	Three-dimensional diffusion	D3	$(3/2)(1-\alpha)^{2/3}[1-(1-\alpha)^{1/3}]^{-1}$	$[1-(1-\alpha)^{1/3}]^2$
11	Contracting sphere	R3	$3(1-\alpha)^{2/3}$	$1-(1-\alpha)^{1/3}$
12	Contracting cylinder	R2	$2(1-\alpha)^{1/2}$	$1-(1-\alpha)^{1/2}$
13	Two-dimensional diffusion	D2	$[-\ln(1-\alpha)]^{-1}$	$(1-\alpha)\ln(1-\alpha)+\alpha$

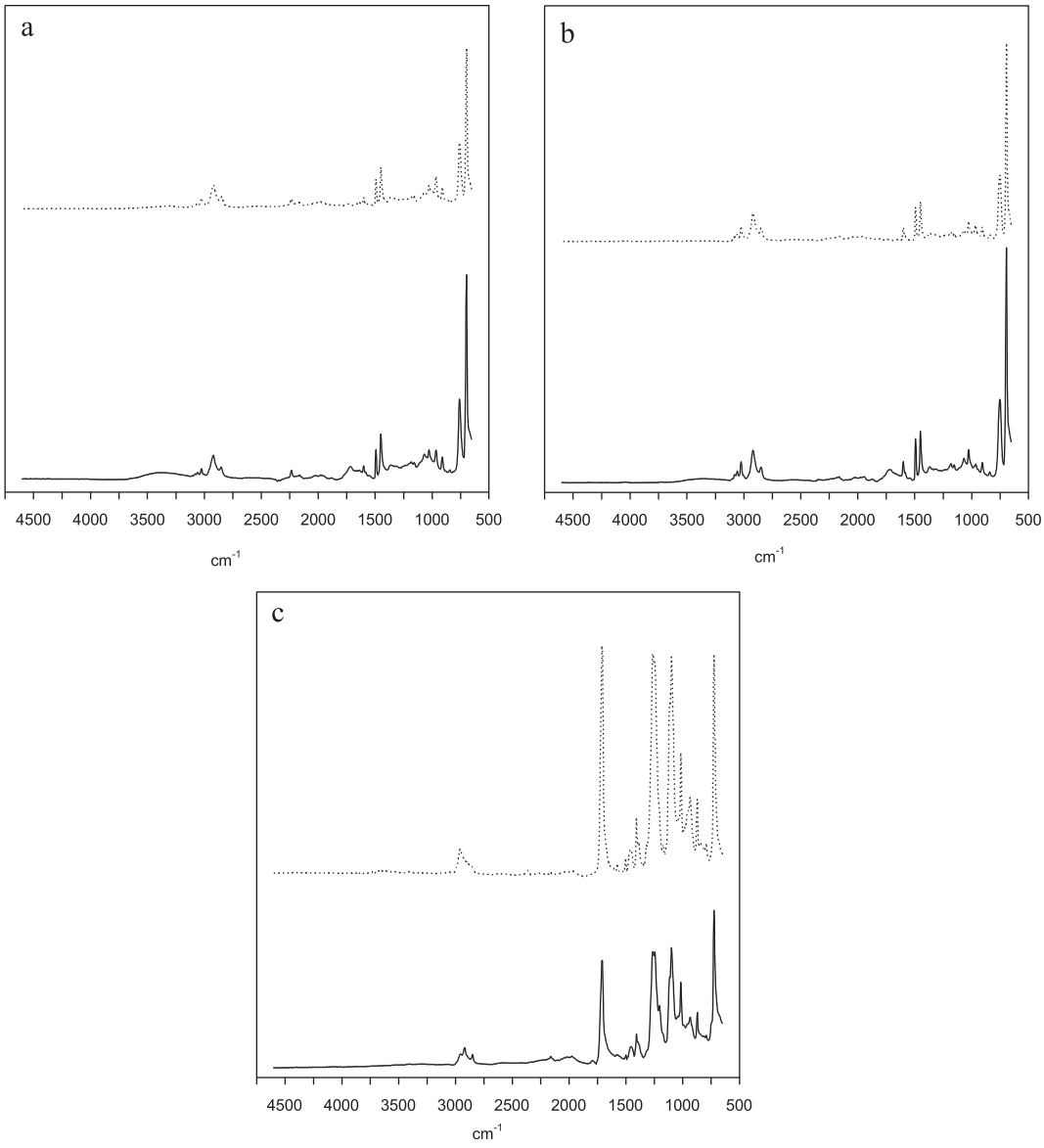

Fig. 1. FTIR spectra of samples: (a) PC, (b) Keyb and (c) black slot. The broken lines relate to the equivalent PS, ABS and PBT virgin polymers, respectively.

$$AIC = N\ln(SS/N) + 2K + 2K(K+1)/(N-K-1) \quad (12)$$

where N is the number of experimental data (11 in this study), embracing $g(\alpha)$ values in the range where is $0.3 < \alpha < 0.8$, with step of 0.05. K is the number of fitting parameters plus 1, and SS is the sum of square differences between the experimental values and the corresponding model calculated values for a fixed value of α. The lower the AIC value the higher chance to select the best model function [43]. This expression was adopted every time the data set number was found to be of the same magnitude order of the fitting parameters, or lower than a few dozen times as much as the K number. When the difference of the AIC numbers associated to a couple of models compared (ΔAIC) was found to be lower than 10, a further discriminating criterion was considered, based on computation of the associated probability P according to the following expression:

$$P = \exp(-0.5\Delta AIC)/[1+\exp(-0.5\Delta AIC)] \quad (13)$$

Once the so-called kinetic triplet is reliably determined the reaction time t_α to achieve a given conversion degree α at a reference temperature T_0 to be determined by integrating Eq. (3) according to the following Eq. (14):

$$t_\alpha(T_0) = g(\alpha)/[A_\alpha \exp(-E_\alpha/RT_0)] \quad (14)$$

where $g(\alpha)$ represents the model function previously selected.

3. Results and discussion

3.1. WEEE characterisation

The FT-IR analysis allowed identifying the polymeric constituents on WEEE plastic samples as reported in Fig. 1a–c. Each figure contains two spectra: the sample (solid line) and the virgin polymer (dotted line). HIPS was identified from the following interpretation of the spectrum reported in Fig. 1a. The bands around 3000–3082 cm^{-1} and at 698–759 cm^{-1} are characteristic of the presence of aromatic ring or substituted phenyl ring; peaks at 910 cm^{-1} (C–H) and 964 cm^{-1} (C=C) correspond to butadiene phase. The peak around 1450–1492 cm^{-1} is related to the

Table 3
Elemental and proximate analysis of WEEE plastic samples and of virgin reference polymers.

WEEE plastic sample	C (%)[a]	H (%)[a]	N (%)[a]	S (%)[a]	O (%)[a]	Cl (%)	Br (%)	Volatile matter (%)	Fixed carbon (%)	Ash (%)
HIPS std	91.0 ± 0.5	9.0 ± 0.1	n.d.	n.d.	–	–	–	n.m.	n.m.	0.14 ± 0.03
ABS std	85.9 ± 0.7	8.0 ± 0.1	5.08 ± 0.04	n.d.	–	–	–	n.m.	n.m.	0.210 ± 0.004
PBT std	65 ± 1	5.5 ± 0.1	n.d.	n.d.	25 ± 2	–	–	n.m.	n.m.	0.20 ± 0.01
PC	90 ± 1	8.5 ± 0.1	n.d.	n.d.	–	–	–	98.7 ± 0.4	0.14 ± 0.05	1.2 ± 0.2
Keyb	84.3 ± 0.3	7.82 ± 0.01	5.0 ± 0.3	n.d.	–	–	–	97.3 ± 0.2	1.0 ± 0.3	1.4 ± 0.3
Black slot	46.9 ± 0.2	3.89 ± 0.02	n.d.	n.d.	20.6 ± 0.7	0.16 ± 0.04	3 ± 1	69.3 ± 0.7	7.9 ± 0.6	22.6 ± 0.8
Real WEEE	85.1 ± 0.5	7.93 ± 0.04	3.2 ± 0.2	n.d.	0.62 ± 0.02	n.d.	n.d	96.5 ± 0.2	0.93 ± 0.09	2.4 ± 0.3

n.d. = non detected; n.m. = not measured.
[a] On dry weight basis.

stretching vibrations of the aromatic ring, while the peak at 1600 cm^{-1} is caused by the stretching vibration of the aromatic carbon–carbon double bond. The spectrum of ABS (Fig. 1b) shows the same bands of HIPS, as it has two monomers in common, with the only exception of the presence of the nitrile group, which absorbs near 2237 cm^{-1}. The presence of PBT in the black slot was revealed by the peak at 1712 cm^{-1}, attributed to the characteristic stretching of carbonyl inside the carbonate functional group. It is worth noting the presence of the absorbance bands due to the aryloxy group (C–O–C), near 1246–1261 cm^{-1}, and those of the alkyl groups at 1408 cm^{-1} and 2897–2958 cm^{-1}. Moreover, the sample FT-IR spectra were compared with the virgin one to estimate differences (if any). The presence of hydroxyl groups in the WEEE housing samples, revealed by the peaks at 1724 cm^{-1} and 3200–3400 cm^{-1} respectively, can be ascribed to the degradation due to ageing oxidation [44]. This phenomenon is not seen in the sample of the Black slot (Fig. 1c), which is installed inside the personal computer.

Results from proximate as well as from ultimate analysis are reported on Table 3 while the HHV and LHV data determined by calorimetric measurements are reported in Table 4. Humidity of all samples (as weight loss at 105 °C) ranged between 0.1% and 0.2% w/w, sign of waterproof material quality ascribable to these WEEE plastics. Fixed carbon is around 1% for all but black slot sample, which nearly achieves 8%. This result suggests that pyrolysis occurring in thermoplastics derived by external cases may convert the whole hydrocarbon content contained in the solid fraction into a fluid shape, whether liquid or gas. The ash content is less than 3% for all examined samples, either the ones coming from housing electric devices and from virgin polymers, with the only exception of the black slot which shows a remarkable high ash content (≥20%). The analysis on other slot typologies taken from PCBs confirmed an ash content of the same magnitude (i.e. a nylon 6.6 slot gave a value of 32%). Elemental analysis of WEEE samples concerning C, H, N, S, O appeared in good agreement with their homologous virgin polymers samples and derivable from the monomer molecular formula. In particular, it is worth noting that N is detected only in ABS samples as a final confirmation of the presence of a nitrile group. Finally, chlorine and bromine were found only in black slot. The measurements of LHV gave results in good agreement with the elemental analysis as it was confirmed by the comparison with the LHV drawn by application of the well-known Dulong-Petit expression [45]:

$$\mathrm{HHV}\left(\mathrm{MJ\cdot kg^{-1}}\right) = 32.959\left(\%\mathrm{C}\right) + 142.915\left[\%\mathrm{H} - \left(\%\mathrm{O}/8\right)\right] + 9.254\left(\%\mathrm{S}\right) - 9\left(\mathrm{HyC}\right) - 2.5\left(\mathrm{HuC}\right) \quad (15)$$

where %C, %H, %O and %S are the elemental content of each material as determined experimentally (expressed in % w/w). Housing samples showed features very similar to those of the virgin polymers, while all analysed parameters concerning the slot sample strongly differ from that of virgin PBT. Deviation in the results of elemental analysis can be ascribed to the presence of high ash content. Indeed, by recalculating the element percentages on an ash-free basis (%C = 63%, %H = 5% and %O = 26%), very close values to virgin PBT were obtained. The high ash content strongly contributes to lower the LHV, which does not exceed 19 MJ kg^{-1}. In spite of what it can be expected, strong clues for the presence of flame retardants were detectable only in slot samples: the significant concentration of bromine, the presence of antimony (Sb_2O_3 is known a flame retardant [46]) measured by EDXRF spectroscopy, as shown in Table 5, and lastly the flame test where the slot burning spontaneously extinguished, in comparison with housing samples which kept burning after removal of the direct flame. The same values for the mixture Real WEEE are reported in Table 3 as well. Aiming at applying a pyrolysis process to mixed plastics, it can be seen that the "dilution" effect offsets the drawbacks of black slot features, like ash content, minor carbon percentage and halogens concentration.

Table 4
Calorimetric analysis of WEEE plastic samples and of virgin reference polymers.

Sample	HHV (MJ kg^{-1})	LHV (MJ kg^{-1})	Dulong-Petit expression LHV (MJ kg^{-1})
HIPS std	41.825 ± 0.005	39.85	40.83
ABS std	39.84 ± 0.05	37.05	37.94
PBT std	25.84 ± 0.06	24.60	23.58
PC	41.06 ± 0.01	39.15	39.93
Keyb	38.91 ± 0.03	37.14	37.18
Black slot	18.98 ± 0.02	18.10	16.37

3.2. Thermal behaviour

The TG/DTG curves of the WEEE plastic samples at the heating rates of 2, 5, 10, 15 K min^{-1} are shown in Fig. 2a–d. As it can be seen, almost all the four materials investigated undergo a two-step pyrolysis process, the main of which, at lower temperatures, occurs in the temperature range from 663 to 693 K, and is accompanied by a weight loss between 80% and 100%. As expected from the characterization results reported in the previous paragraph, plastic housing samples (PC and Keyb) show a similar behaviour, substantially the same of those of their corresponding virgin polymers (TG/DTG curves not shown), since no residue is present after 873 K. The second decomposition step concerning PC and Keyb samples may be attributed to the loss of butadiene as generally known.

Table 5
EDRXF analysis of the ashes of black slot sample.

Ca	Sb	Si	Fe	Cs	Zn	Sr	Cr	Ni	Se	Cu
39.0%	34.6%	18.3%	3.0%	1.9%	1.1%	0.8%	0.7%	0.3%	0.2%	0.2%

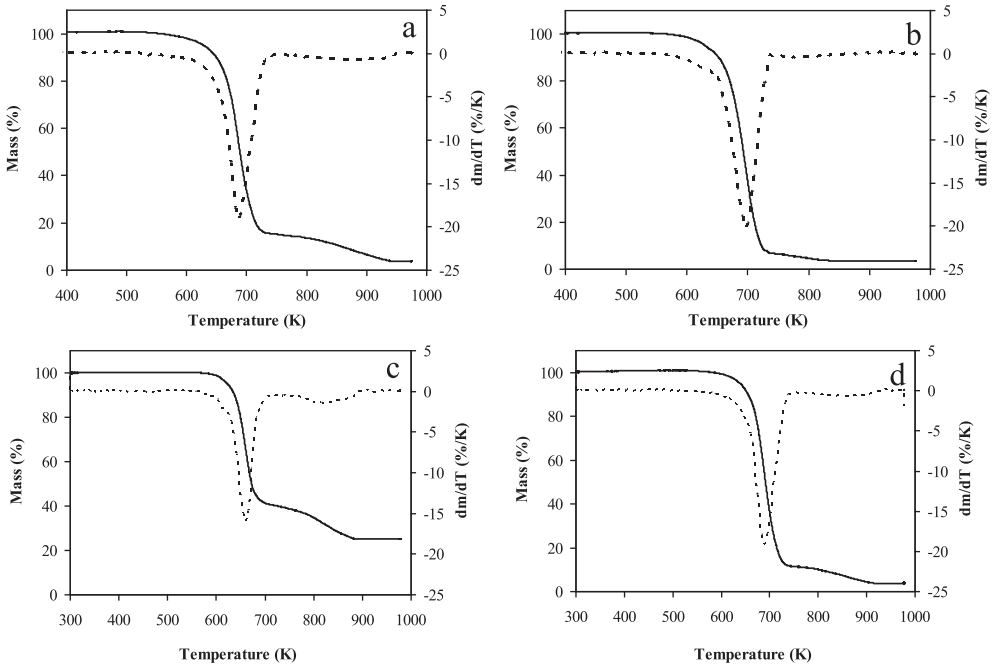

Fig. 2. TG (solid line) and DTG (broken line) curves of WEEE plastic samples at 10 K min^{-1} for: a) Keyb, b) PC, c) Black slot, d) Real WEEE.

Black slot sample shows on the other side a marked difference in composition with respect to PBT concerning the residue (20% higher than that of PBT).

Finally, pyrolysis was applied to Real WEEE sample, giving a shape of DTG curve very similar to that of Keyb, which is the main component. On the other hand, ABS shows a degradation process very similar to that of other styrene derivatives. We can observe that with addition of small amount of a condensation polymer (PBT) (as low as 3% by weight) the degradation curves of styrene-based polymers (ABS and HIPS) did not change appreciably. Therefore, no significant interactions (at least at these dilutions) have to be considered between these two polymers categories during the occurrence of their thermal degradation. According to our knowledge no such behaviour (PBT- styrene-based polymers interactions) was observed. In any case, this work took into consideration the kinetic study applied only to the temperature region of the first DTG peak corresponding to the main or unique weight loss of the decomposition process. The mass conversion into volatiles shows similar behaviour for all the applied heating rates (Fig. 3a–d). Similar shapes of the α *vs*. temperature curves confirms

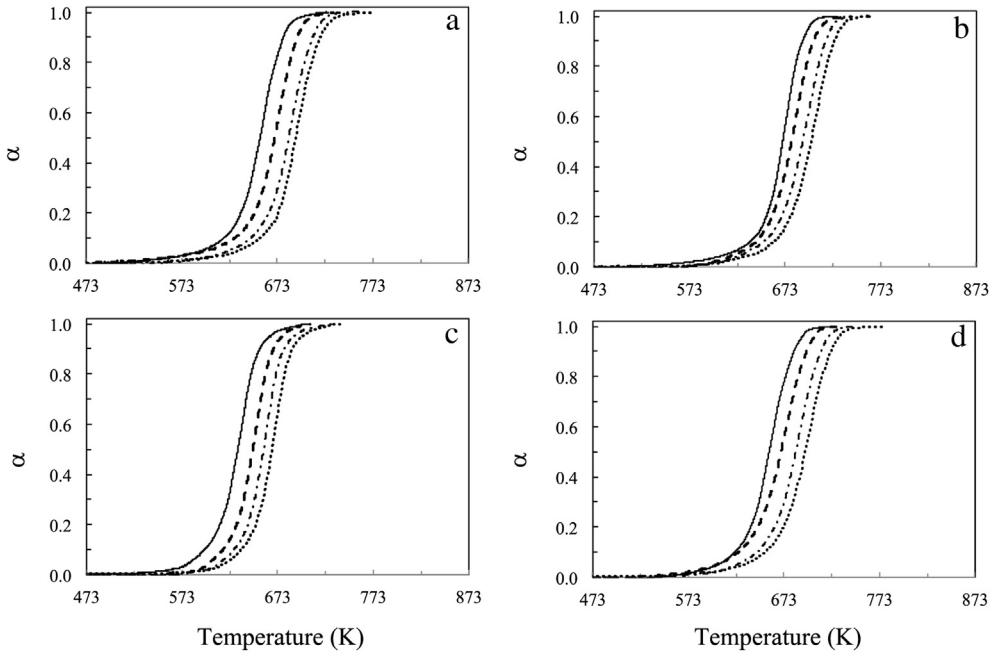

Fig. 3. Conversion plots for the first step of pyrolysis occurring in the WEEE plastic samples at different heating rates (from 2 to 15 K min^{-1}, from left to right) for: a) Keyb, b) PC, c) Black slot, d) Real WEEE.

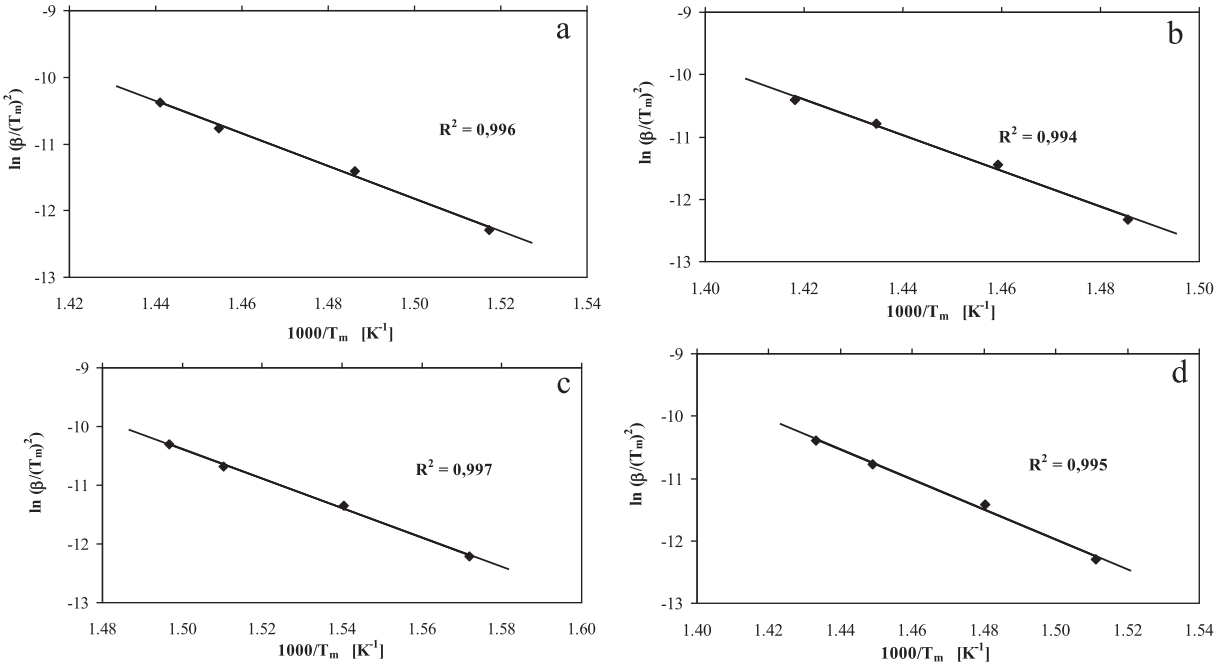

Fig. 4. Kissinger plots for WEEE plastic samples: a) Keyb, b) PC, c) Black slot, d) Real WEEE.

the existence of the same single or sequence of mechanisms regardless the heating rate, allowing the adoption of model-free methods. During the analysis, at low heating rate, a larger instantaneous thermal energy is provided in the system and a longer time may be required for the purge gas to reach equilibrium with the furnace temperature. On the other hand at the same time and in the same temperature region, higher heating rate has a short reaction time and the temperature needed for the sample to decompose is also higher.

3.3. Kinetic analysis of pyrolysis

Fig. 3 shows the temperature dependence of conversion plots at different heating rates for the main pyrolysis process at lower temperatures. As expected, the shapes of these curves are very similar regardless the heating rate, thus suggesting that the reaction mechanism is not influenced by the heating rate (requirement of OFW and other isoconversional methods).

Kissinger plot for the first pyrolysis process occurring in all the examined samples is reported in Fig. 4a–d allowing the determination of E_a by applying Eq. (5). Each experimental point is the result of three replicates, which showed a standard deviation values between 0.01 and 0.3. The values of activation energy associated to the pyrolysis of Keyb, Black slot and Real WEEE are 208 ± 8, 216 ± 8 and 208 ± 8 kJ mol^{-1}, respectively. No significant differences can be considered among these values since they fall within the estimated uncertainties, while a higher E_a value (249 ± 8 kJ mol^{-1}) is found for the process occurring in the PC sample.

Kinetic parameters associated to the thermally activated pyrolysis of each WEEE sample obtained by OFW method were calculated according to Eq. (7) at any value of α between 0.05 and 0.95. Fig. 5 shows each the regression straight line derived by plotting $\ln(\beta_i)$ *vs.* $(T_{\alpha,i})^{-1}$ at each fixed value of α. Fig. 6 shows the conversion dependencies of E_a according to the OFW method together with the E_a value calculated according to the Kissinger method (reported as horizontal dashed lines). As far as pyrolysis of the four samples is concerned, one can observe that E_a is not constant in the whole range of conversion, which means that at least two mechanisms of decomposition may be involved. Starting from approximately $\alpha = 0.4$ onwards, the E_a values are practically constant and the average value (E_0) of those found in the range of α between 0.3 and 0.8 is in close agreement with the one calculated using the Kissinger method, as it can be observed in Table 6. It is difficult to make comparisons between these results and those ones found in similar studies carried out on the same commercial polymers, due to the wide range of E_a values reported by several authors in their papers [25–30,47–49]. However, some E_a values of pyrolysis occurred in virgin polymers reported in literature do not differ significantly from the corresponding found in this study. In particular, two values for ABS (179.3 and 175.8 kJ mol^{-1} [28,47]) are only slightly lower than the average value of Keyb in Table 6, while other E_a values found for pyrolysis of ABS depend remarkably on the heating rate considered [26], probably due to the method used (model-fitting) that sometimes may provide unreliable results [41]. Literature E_a data on pyrolysis of virgin HIPS spread over a wide range, but the values determined by Liu and coworkers [27] agree well with those found in this study (within the estimated uncertainties). E_a mean value for pyrolysis of PBT is slightly higher than literature ones [29,30] probably because of the presence of a high content of additives in the Black slot sample (Table 3). Therefore, the presence of scattered values of Arrhenius parameters taken from literature may depend both on the different operating conditions adopted (type of carrier gas, flow rate, heating rate) and the misuse adopted by some authors of simple first order kinetic model to interpret the experimental data. As Westerhout and co-workers pointed out in their review [25], the values of E_a for PS vary from 83 to 440 kJ mol^{-1}. In addition, differences in the values of Arrhenius parameters can be attributed to the different composition of polymer components in the plastics contained in commercial small appliances. In particular, the fraction of each monomer in both commercial ABS and HIPS copolymers spreads over wide ranges: the fraction of 1,3-butadiene monomer in commercial ABS span from 10 to 40% w/w, and commercial HIPS copolymers have usually

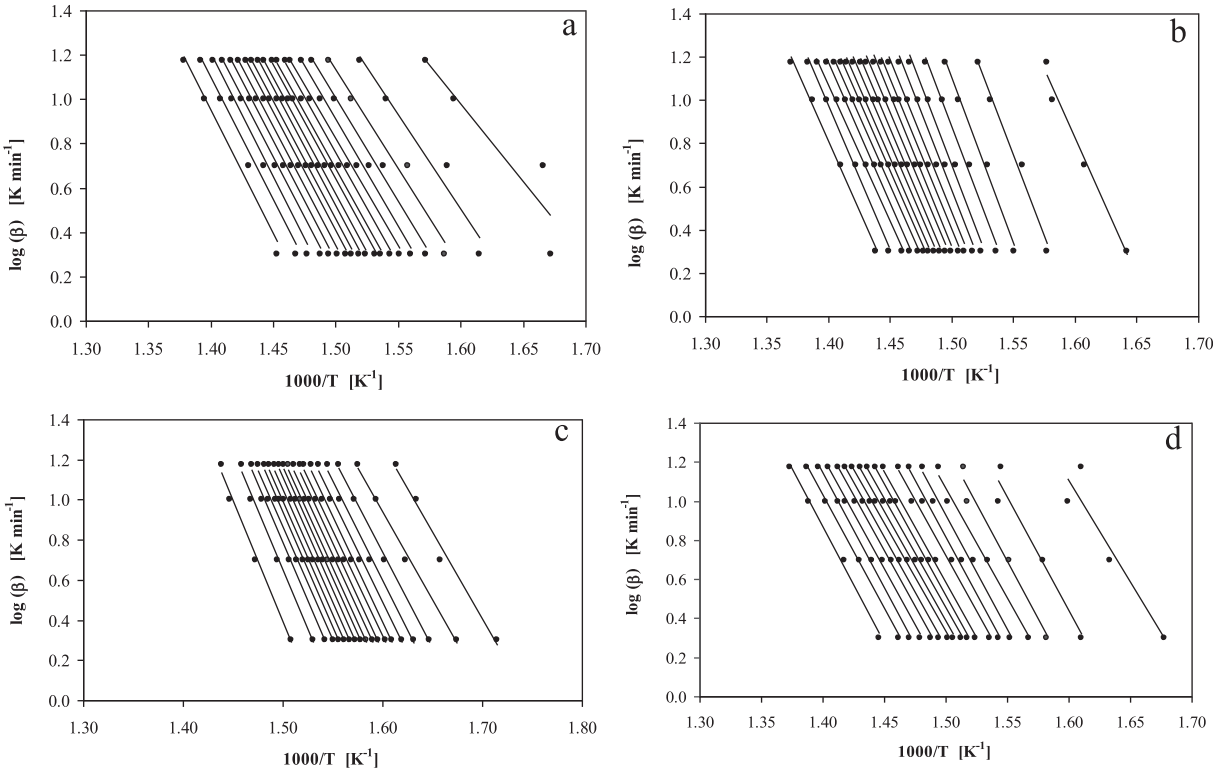

Fig. 5. OFW plots of the examined samples for different values of conversion (from 0.05 to 0.95 from right to left): a) Keyb, b) PC, c) Black slot, d) Real WEEE.

variable concentration (between 5 and 20% w/w) of a styrene–butadiene rubber [50].

To determine the value of A (at each value of α) regardless the knowledge of the reaction model, the method already described in "Materials and Methods" section, was used for the four samples. The Coats-Redfern method [42] was not used to get a further confirmation of E_a values, because model-fitting methods based on a single heating rate are known to provide unreliable kinetic results

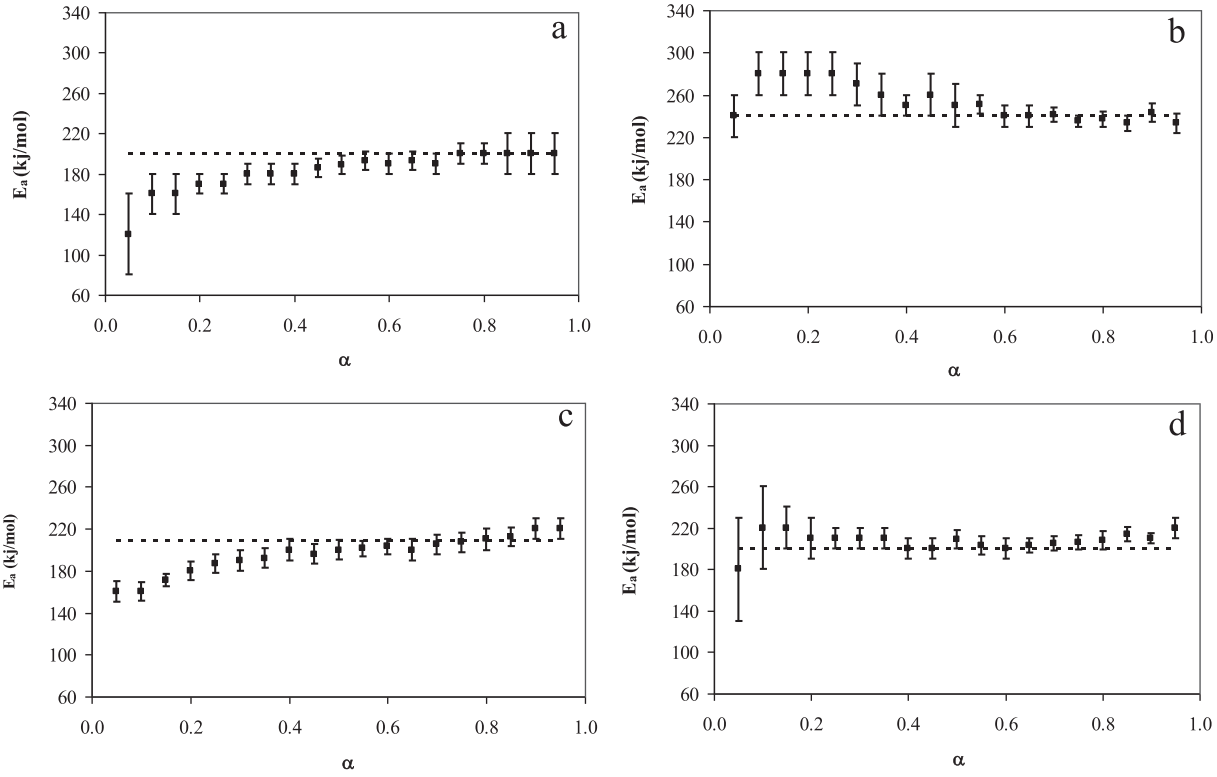

Fig. 6. Conversion dependencies of activation energy for the first step of pyrolysis according to the Flynn-Wall method for WEEE plastic samples: a) Keyb, b) PC, c) Black slot, d) Real WEEE. The broken line represents the E_a value obtained by the Kissinger method.

Table 6
Average values of Arrhenius parameters derived by their isoconversional trends, used in Eq. (11) to select the best among the 13 models considered.

	E_0 (kJ mol^{-1})	ln(A_0/min^{-1})
Keyb	198 ± 6	32 ± 1
PC	259 ± 11	43 ± 1
Black slot	210 ± 7	35 ± 1
Real WEEE	214 ± 6	35 ± 1

[51]. The method makes use of the so-called compensation effect that is observed when a model fitting method is applied to a single heating rate run for the different model functions (13 models in this study, whose mathematical expressions for $f(\alpha)$ and $g(\alpha)$ are given in Table 2). The compensation effect is shown in Fig. 7 for the thermal degradation of real WEEE sample with an excellent linear fit ($R^2 > 0.998$) of the trend ln$A$ vs. E_a. Similar behaviours are observed for the trends ln$A$ vs. E_a concerning the thermal degradation of the other examined WEEE plastic samples. Once the values of the regression coefficients of Eq. (9) a and b are determined at each heating rate the corresponding mean values, $\langle a \rangle$ and $\langle b \rangle$, were used in Eq. (10) to determine the conversion dependency of ln$A$ (ln$A$ vs. α).

Since no significant changes of activation energy was observed in all WEEE samples studied in the range $0.3 < \alpha < 0.8$ (Fig. 6), the most suitable model function was selected from the best agreement between the $g(\alpha)$ values reconstructed with those calculated using the expressions in Table 2 according to a procedure similar to that reported in more detail elsewhere [52] and adopted in recent studies [53,54]. For this purpose, the average values of Arrhenius parameters, E_0 and lnA_0, calculated from their conversion dependency trends in the range $0.3 < \alpha < 0.8$ were inserted in Eq. (11). Once the numerical trends of $g(\alpha)$ were reconstructed as a function of α by integrating Eq. (11) for all pyrolysis processes, they were compared in Fig. 8 with the theoretical ones determined according to the expression given in Table 2. At a first sight, the best reaction models for thermal degradation of the real WEEE sample as well as for that of the WEEE plastic samples identified on the basis of the best match between reconstructed and calculated (theoretical) conversion dependency of $g(\alpha)$ (Fig. 5) seem to be R3 and D2.

In order to make a final choice between the two candidate model functions that best describe the pyrolysis process of Keyb, PC, Black slot and Real WEEE the values of AIC determined according to Eq. (11) were reported in Table 7. As expected, the lowest values (significantly lower than those of all the other functions), which correspond to the best function, were found to be R3 and D2 (in bold in Table 7), but the values cannot be considered significantly different (from a statistical point of view) to discriminate

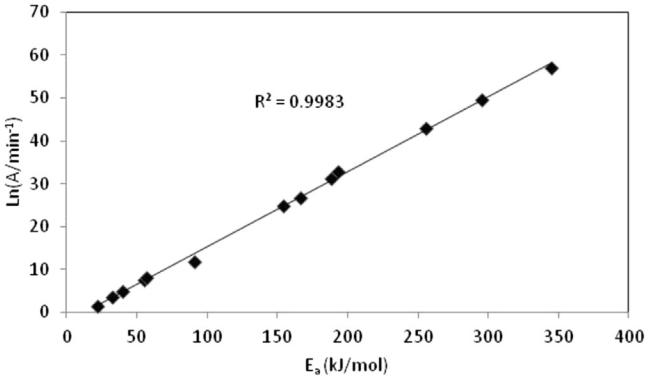

Fig. 7. Compensation effect for the real WEEE sample at a heating rate of 10 K min^{-1}.

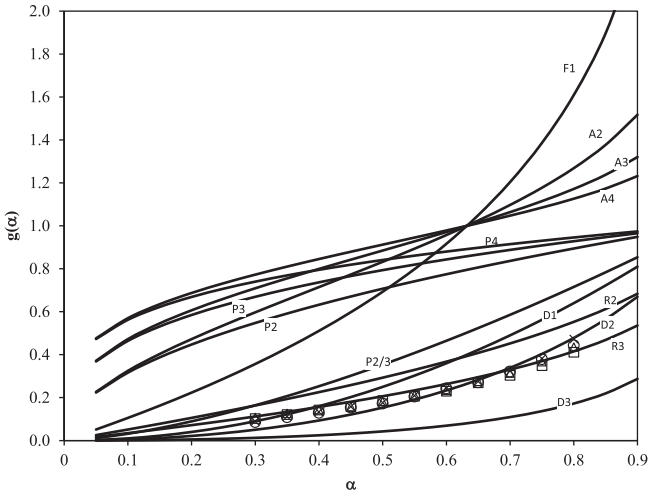

Fig. 8. Experimental data for all WEEE samples at 10 K min^{-1} and the theoretical kinetic models defined in Table 6.

between them. Therefore, the percentage of chance that one of the two functions could be the best suitable one was calculated according to Eq. (13) and the values given in Table 8. A final attribution is possible with a high degree of certainty for pyrolysis of Keyb, PC and real WEEE (R3), while for the Black slot sample the uncertainty between the R3 and D2 models cannot be solved using this approach (they seem to be equivalent). Similar cases cannot be completely solved using a mathematical approach, but it should be recommended to carry out further experimental work, including infrared or mass spectroscopy measurements, morphology study using SEM or TEM on the intermediates and final products. According to our expectations, the real WEEE sample was found to follow the same behaviour of styrene-based samples representing the most abundant components within the mixture.

Finally, the temperature dependency of reaction time was determined according to Eq. 14 at $\alpha = 0.6$, which corresponds to the

Table 7
Values of AIC determined according to Eq. (12) for selection of the best model function for pyrolysis of Keyb, PC, Black slot and Real WEEE samples

Reaction model	Keyb	PC	Black slot	Real WEEE
P4	−11.50	−11.70	−11.73	−11.51
P3	−13.07	−13.28	−13.32	−13.08
P2	−16.18	−16.44	−16.52	−16.23
P2/3	−35.43	−36.22	−36.90	−36.01
D1	−46.03	−47.46	−49.19	−47.48
F1	−8.96	−9.21	−9.44	−9.14
A4	−8.50	−8.69	−8.75	−8.54
A3	−8.90	−9.09	−16.97	−8.95
A2	−9.41	−9.62	−11.21	−9.50
D3	−41.31	−40.31	−42.49	−40.67
R3	**−85.77**	**−88.19**	**−80.76**	**−83.75**
R2	−48.16	−49.42	−50.11	−48.78
D2	**−71.14**	**−73.83**	**−81.28**	**−78.64**

The lowest negative values that enable to select the best model functions are given in bold.

Table 8
Percentage of chance that the candidate models previously selected (R3 or D2) could be the best suitable one according to Eq. (13).

Reaction model	R3	D2
Keyb	99	1
PC	99	1
Black slot	44	56
Real WEEE	93	7

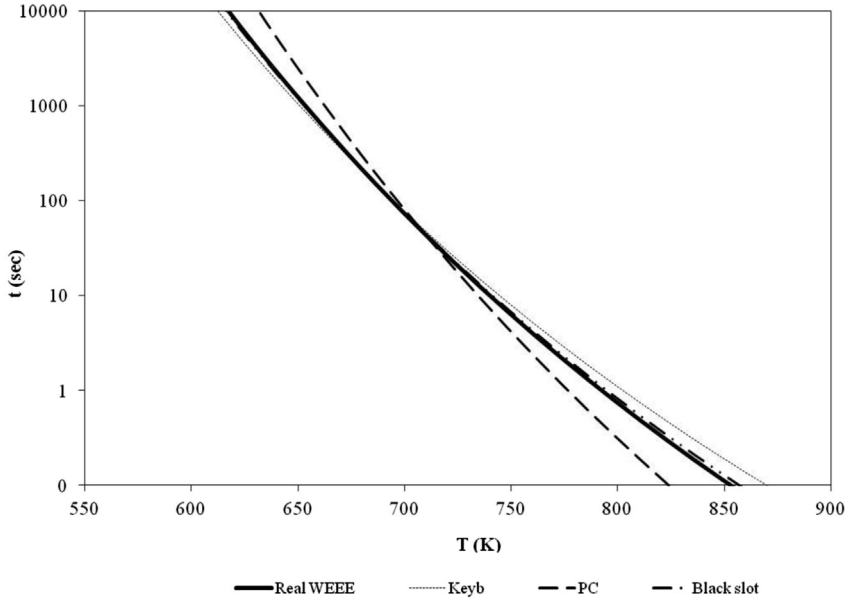

Fig. 9. Temperature dependency of pyrolysis times for the WEEE plastic samples at $\alpha = 0.6$.

inflection point of the mass loss in the TG curve (i.e., the maximum decomposition rate) occurring in all samples regardless the heating rate, using the $g(\alpha)$ function corresponding to the model R3 for pyrolysis of all WEEE samples. Moreover, in the case of Black slot the computation of $t_{0.6}(T_0)$ as a function of temperature T_0 was made using both models, even if the choice of R3 instead of D2 implies a difference of only 35 s to achieve the maximum decomposition rate ($\alpha = 0.6$) at 673 K. At this extent of conversion, this results can be ascribed to the practical superimposition of the trends of $g(\alpha)$ *vs.* α regarding the two mentioned models with the numerical one calculated by⧹ experimental data in Fig. 9. All the reaction temperature-time curves reported in Fig. 9, showed for the different WEEE plastics the same trend and shape: below 550 K the decomposition reaction of all samples has a virtual infinite time. Time decreases exponentially and at 700 K the slowest process (occurring in Keyb) shows a decomposition time of about 26 s. It can be seen that the curve related to the PC sample shows the highest slope, which corresponds to the highest E_a value. On the other hand, up to 650 K the PC sample is associated to the slowest thermal degradation, which confirms the thermal stability of this polymer, as it is a high impact styrene. As expected, the real WEEE sample showed an intermediate trend with respect to the others curves. Moreover, ABS and HIPS (coded as PC and Keyb, respectively) have styrene as the main monomer. These curves allow to establish the temperature above which kinetics is not more the limiting factor of the pyrolysis process.

4. Conclusions

This paper reports the identification and characterization of some thermoplastic components of WEEE through the study of their thermal behaviour when they are subjected to a pyrolysis process. This issue was dealt with by the modelling of highly heterogeneous thermoplastic composition through a simplified ternary mixture of the three main polymeric constituents, coming from small household appliances of WEEE treatment plants. The main polymer components contained in the mixed plastic waste samples coming from external cases and PCBs of small appliances exhibit similar thermal behaviour.

Kinetic analysis of the pyrolysis process carried out with both the Kissinger and OFW methods enabled to determine reliable kinetic triplet and lifetime at given extent of conversion and temperature for some polymer components and a real WEEE sample. For all components at the set operating conditions of pyrolysis, residue was found to be of the same ash percentage, in consequence of which, the process led to an almost complete separation of the organic fraction. This may represent an advantage both to manage the process for the scale-up and to better valorize the plastic waste obtaining an oil-rich fraction for further synthesis uses.

References

[1] Final proposal COM. 810 for a directive of the European parliament and of the council on waste electrical and electronic equipment (WEEE); 2008.
[2] Directive 2012/19/EU of the European parliament and of the council of 4 July 2012 on waste electric and electronic equipment (WEEE).
[3] Cui J, Forssberg E. Mechanical recycling of waste electric and electronic equipment: a review. J Hazard Mater 2003;B99:243–63.
[4] Decreto Legislativo 36/03, Attuazione della direttiva 1999/31/CE relativa alle discariche di rifiuti, Gazzetta Ufficiale n. 59, 12 marzo 2003-Supplemento Ordinario n. 40.
[5] Heerman C, Schwager FJ, Whiting KJ. Pyrolysis & gasification of waste "a worldwide technology and business review". Uley, Gloucestershire, England: Juniper Consultancy Services, Ltd.; 2001.
[6] De Marco I, Caballero BM, Chomón MJ, Laresgoiti MF, Torres A, Fernandez G, et al. Pyrolysis of electrical and electronic wastes. J Anal Appl Pyrolysis 2008;82:179–83.
[7] Riess M, Ernst T, Popp R, Mueller B, Thoma H, Vierle O, et al. Analysis of flame retarded polymers and recycling materials. Chemosphere 2000;40:937–47.
[8] Directive 2011/65/EU of the European Parliament and of the Council of 8 June 2011 on the restriction of the use of certain hazardous substances in electrical and electronic equipment (RoHS Directive).
[9] Brandrup J. Recycling and recovery of plastics. Munich: Hanser Publishers; 1996.
[10] Heikkinen JM, Hordijk JC, de Yong W, Spliethoff H. Thermogravimetry as a tool to classify waste components to be used for energy generation. J Anal Appl Pyrolysis 2004;71:883–900.
[11] Guo Q, Yue X, Wuang M, Liu Y. Pyrolysis of scrap printed circuit board plastic particles in a fluidized bed. Powder Technol 2010;198:422–8.
[12] Porteous A. Energy from waste direct combustion – a state of the art emissions review with an emphasis on public acceptability. Appl Energy 2001;70:157–67.
[13] Helsen L, van den Bulck E. Review of disposal technologies for chromate copper arsenate (CCA) treated wood waste, with detailed analyses of thermochemical conversion processes. Environ Pollut 2005;134:301–14.

[14] De Marco I, Caballero BM, Cabrero MA, Laresgoiti MF, Torres A, Chomón MJ. Recycling of automobile shredder residues by means of pyrolysis. J Anal Appl Pyrolysis 2007;79:403–8.
[15] De Marco Rodriguez I, Laresgoiti MF, Cabrero MA, Torres A, Chomón MJ, Caballero BM. Pyrolysis of scraps tyres. Fuel Proc Technol 2001;72:9–22.
[16] Fantozzi F, Desideri U. Micro scale slow pyrolysis rotary kiln for syngas and char production from biomass and waste, 2nd world conference on biomass for energy, industry and climate protection, 10–14 May 2004, Rome, Italy.
[17] De Angelis Curtis S, Kubiak M, Kurdziel K, Materazzi S, Vecchio S. Crystal structure and thermoanalytical study of a cadmium(II) complex with 1-allylimidazole. J Anal Appl Pyrolysis 2010;87:175–9.
[18] Papadopoulos C, Kantiranis N, Vecchio S, Lalia-Kantouri M. Lanthanide complexes of 3-methoxy-salicylaldehyde Thermal and kinetic investigation by simultaneous TG/DTG–DTA coupled with MS. J Therm Anal Calorim 2010;99:931–8.
[19] Vecchio S, Campanella L, Nuccilli A, Tomassetti M. Kinetic study of thermal breakdown of triglycerides contained in extra-virgin olive oil. J Therm Anal Calorim 2008;91:51–6.
[20] Simon P. Isoconversional methods: fundamentals, meaning and application. J Therm Anal Calorim 2004;76:123–32.
[21] Kantarelis E, Yang W, Blasiak W, Forsgren C, Zabaniotou A. Thermochemical treatment of E-waste from small household appliances using higly pre-heated nitrogen-thermogravimetric investigation an pyrolysis kinetics. Appl Energy 2011;88:922–9.
[22] Barontini F, Cozzani V. Formation of hydrogen bromide and organo-brominated compounds in the thermal degradation of electronic boards. J Anal Appl Pyrolysis 2006;77:41–55.
[23] Blanco I, Abate L, Bottino FA. Variously substituted phenyl hepta cyclopentyl – polyhedral oligomeric silsesquioxane (ph,hcp-POSS)/Polystyrene (PS) nanocomposites. The influence of substituents on the thermal stability. J Therm Anal Calorim 2013;112:421–8.
[24] Blanco I, Bottino FA, Bottino P. Influence of symmetry/asymmetry of the nanoparticles structure on the thermal stability of polyhedral oligomeric silsesquioxane/polystyrene nanocomposites. Polym Compos 2012;33(11):1903–10.
[25] Westerhout RWJ, Waanders J, Kuipers JAM, van Swaaij WPM. Kinetics of the low-temperature pyrolysis of polyethene, polypropene, and polystyrene modeling, experimental determination, and comparison with literature models and data. Ind Eng Chem Res 1997;36:1955–64.
[26] Encinar JM, Gonzales JF. Pyrolysis of synthetic polymers and plastic wastes. Kinetic study. Fuel Proc Technol 2008;89(7):678–86.
[27] Liu H, Kong Q, Cheng Y, Cao G. Thermal decomposition kinetics of high impact polystyrene/organo Fe-montmorillonite nanocomposites. Chin J Chem 2012;30:1594–600.
[28] Yang M. The thermal degradation of acrylonitrile-butadiene-styrene terpolymer under various gas conditions. Polym Test 2000;19:105–10.
[29] Pérez-Maqueda LA, Perejón A, Criado JM, Sánchez-Jiménez PE. A new model for the kinetic analysis of thermal degradation of polymers driven by random scission. Polym Degr Stab 2010;95:733–9.
[30] Al-Mulla A, Mathew J, Al-Omairi L, Bhattacharya S. Thermal decomposition of tricomponent polyester/polycarbonate systems. Polym Eng Sci 2011;51:2335–44.
[31] Akaike H. A new look at the statistical model identification. IEEE Trans Autom Control 1974;19:716–23.
[32] Saha B, Ghoshal AK. Model-fitting methods for evaluation of the kinetics triplet during thermal decomposition of poly(ethylene terephthalate) (PET) soft drink bottles. Ind Eng Chem Res 2006;45(23):7752–9.
[33] Motulsky HJ, Christopoulos A. Fitting models to biological data using linear and nonlinear regression. New York: Oxford University Press; 2003, ISBN 0195171802. p. 143–8.
[34] Dimitrakakis E, Janz A, Bilitewski B, Gidarakos E. Small WEEE: determining recyclables and hazardous substances in plastics. J Hazard Mater 2009;161:913–9.
[35] Schlummer M, Gruber L, Maurer A, Wolz G, Van Eldik R. Characterisation of polymer fractions from waste electrical and electronic equipment (WEEE) and implications for waste management. Chemosphere 2007;67:1866–76.
[36] CEN/TS 15408:2006. Solid recovered fuels - methods for the determination of sulphur (S), chlorine (Cl), fluorine (F) and bromine (Br) content; 2006.
[37] Kissinger H. Reaction kinetics in differential thermal analysis. Anal Chem 1957;29:1702–6.
[38] Ozawa T. A new method of analyzing thermogravimetric data. Bull Chem Soc Jpn 1965;38(11):1881–6.
[39] Flynn JH, Wall LA. A quick, direct method for the determination of activation energy from thermogravimetric data. Polym Lett 1966;4:323–8.
[40] Doyle CD. Kinetic analysis of thermogravimetric data. J Appl Polym Sci 1961;5:285–92.
[41] Vyazovkin S, Burnham AK, Criado JM, Pérez-Maqueda LA, Popescu C, Sbirrazzuoli N. ICTAC kinetics committee recommendations for performing kinetic computations on thermal analysis data. Thermochim Acta 2011;520:1–19.
[42] Coats AW, Redfern JP. Kinetic parameters for thermogravimetric data. Nature 1964;201:68–9.
[43] Burnham KP, Anderson DR. Model selection and multimodel inference. A practical information approach. 2nd ed. Springer; 2002.
[44] Tiganis BE, Burn LS, Davis P, Hill AJ. Thermal degradation of acrylonitrile–butadiene–styrene (ABS) blends. Polym Degrad Stab 2002;76:425–34.
[45] Petit A-T, Dulong P-L. Recherches sur quelques points importants de la théorie de la chaleur. Ann Chim Phys 1819;10:395–413.
[46] Jakab E, Uddin MA, Bhaskar T, Sakata Y. Thermal decomposition of flame-retarded high impact polystyrene. J Anal Appl Pyrolysis 2003;68-69:83–99.
[47] Hsing-Yuan Y, Feng-Shyang L, Mu-Hoe Y. Test method thermal degradation of polysulfones. VI: evaluation of thermal pyrolysis of acrylonitrile-butadiene-styrene terpolymer. Polym Test 2003;22:31–6.
[48] Zeng WR, Chow WK, Huo R, Yao B, Li YZ. The degradation kinetic study of polystyrene by a combination of non-isothermal differential and integral methods. Polym Mater Sci Eng Chin 2006;22(5):162–5.
[49] Grause G, Ishibashi J, Kameda T, Bhaskar T, Yoshioka T. Kinetic studies of the decomposition of flame retardant containing high-impact polystyrene. Polym Degr Stab 2010;95:1129–37.
[50] Beyler CL, Hirschler MM. Thermal decomposition of polymers. In: Drysdale D, Beyler CL, Walton WD, Di Nenno PJ, editors. Chapter 7 in the SFPE handbook fire protection engineering. 3rd ed. Quincy MA: NFPA; 2002.
[51] Vyazovkin S, Wight CA. Model-free and model-fitting approaches to kinetic analysis of isothermal and nonisothermal data. Thermochim Acta 1999;340–341:53–68.
[52] Vecchio S, Di Rocco R, Ferragina C. Kinetic analysis of the oxidative decomposition in γ-zirconium and γ-titanium phosphate intercalation compounds. The case of 2,2'-bipyridyl and its copper complex formed in situ. Thermochim Acta 2008;467:1–10.
[53] Vecchio S, Materazzi S, Wo LW, De Angelis Curtis S. Thermoanalytical study of imidazole-substituted coordination compounds: Cu(II)- and Zn(II)-complexes of bis(1-methylimidazol-2-yl)ketone. Thermochim Acta 2013;568:31–7.
[54] Materazzi S, Vecchio S, Wo LW, De Angelis Curtis S. Thermoanalytical studies of imidazole-substituted coordination compounds. Mn(II)-complexes of bis(1-methylimidazol-2-yl)ketone. J Therm Anal Calorim 2011;103:59–64.